

Basics of Semiconductor and Spin Physics

M.I. Dyakonov

This introductory chapter is mainly addressed to readers new to the field. In Sect. 1.1 a brief review of the historical roots of the current research is given. Section 1.2 describes various spin interactions. Section 1.3 is a mini textbook on semiconductor physics designed for beginners. A short overview of spin phenomena in semiconductors is given in Sect. 1.4. Finally, Sect. 1.5 presents the topics discussed in the chapters to follow.

1.1 Historical Background

The first step towards today's activity was made by Robert Wood in 1923/1924 when even the notion of electron spin was not yet introduced. In a charming paper [1] Wood and Ellett describe how the initially observed high degree of polarization of mercury vapor fluorescence (resonantly excited by polarized light) was found to diminish significantly in later experiments. "It was then observed that the apparatus was oriented in a different direction from that which obtained in earlier work, and on turning the table on which everything was mounted through ninety degrees, bringing the observation direction East and West, we at once obtained a much higher value of the polarization." In this way Wood and Ellett discovered what we now know as the Hanle effect, i.e., depolarization of luminescence by transverse magnetic field (the Earth's field in their case). It was Hanle [2] who carried out detailed studies of this phenomenon and provided the physical interpretation.

The subject did not receive much attention until 1949 when Brossel and Kastler [3] initiated profound studies of optical pumping in atoms, which were conducted by Kastler and his school in Paris in the 1950s and 1960s. (See Kastler's Nobel Prize award lecture [4].) The basic physical ideas and the experimental technique of today's "spintronic" research originate from these seminal papers: creation of a non-equilibrium distribution of atomic angular moments by optical excitation, manipulating this distribution by applying *dc* or *ac* fields, and detecting the result by

studying the luminescence polarization. The relaxation times for the decay of atomic angular moments can be quite long, especially when hyperfine splitting due to the nuclear spin is involved.

A number of important applications have emerged from these studies, such as gyroscopes and hypersensitive magnetometers, but in my opinion, the knowledge obtained is even more valuable. The detailed understanding of various atomic processes and of many aspects of the interaction between light and matter was pertinent to the future developments, e.g., for laser physics.

The first experiment on the optical spin orientation of electrons in a semiconductor (Si) was done by Georges Lampel [5] in 1968, as a direct application of the ideas of optical pumping in atomic physics. The greatest difference, which has important consequences, is that now these are the free conduction band electrons (or holes) that get spin-polarized, rather than electrons bound in an atom. This pioneering work was followed by extensive experimental and theoretical studies mostly performed by small research groups at Ioffe Institute in St. Petersburg (Leningrad) and at Ecole Polytechnique in Paris in the 1970s and early 1980s. At the time this research met with almost total indifference by the rest of the physics community.

1.2 Spin Interactions

This section serves to enumerate the possible types of spin interactions that can be encountered in a semiconductor.

The existence of an electron spin, $s = 1/2$, and the associated magnetic moment of the electron, $\mu = e\hbar/2mc$, has many consequences, some of which are very important and define the very structure of our world, while others are more subtle, but still quite interesting. Below is a list of these consequences in the order of decreasing importance.

1.2.1 The Pauli Principle

Because of $s = 1/2$, the electrons are fermions, and so no more than one electron per quantum state is allowed. Together with Coulomb law and the Schrödinger equation, it is this principle that is responsible for the structure of atoms, chemical properties, and the physics of condensed matter, biology included. It is interesting to speculate what would our world look like without the Pauli principle and whether any kind of life would be possible in such a world! Probably, only properties of the high-temperature, fully ionized plasma would remain unchanged. Note that the Pauli exclusion principle is not related to any interaction: if we could switch off the Coulomb repulsion between electrons (but leave intact their attraction to the nuclei), no serious changes in atomic physics would occur, although some revision of the Periodic Table would be needed.

Other manifestations of the electronic spin are due to interactions, either electric (the Coulomb law) or magnetic (related to the electron magnetic moment μ_B).

1.2.2 Exchange Interaction

It is, in fact, the result of the electrostatic Coulomb interaction between electrons, which becomes spin-dependent because of the requirement that the wave function of a pair of electrons be anti-symmetric with respect to the interchange of electron coordinates and spins. If the electron spins are parallel, the coordinate part of the wave function should be antisymmetric: $\psi_{\uparrow\uparrow}(\mathbf{r}_2, \mathbf{r}_1) = -\psi_{\uparrow\uparrow}(\mathbf{r}_1, \mathbf{r}_2)$, which means that the probability that two electrons are very close to each other is small compared to the opposite case, when the spins are antiparallel and accordingly their coordinate wave function is symmetric. Electrons with parallel spins are then better separated in space, so that their repulsion is less and consequently the energy of the electrostatic interaction for parallel spins is lower.

The exchange interaction is responsible for ferromagnetism. In semiconductors, it is normally not of major importance, except for magnetic semiconductors (like CdMnTe) and for the semiconductor-ferromagnet interface.

1.2.3 Spin–Orbit Interaction

If an observer moves with a velocity \mathbf{v} in an external electric field \mathbf{E} , he will see a magnetic field $\mathbf{B} = (1/c)\mathbf{E} \times \mathbf{v}$, where c is the velocity of light. This magnetic field acts on the electron magnetic moment. This is the physical origin of the spin–orbit interaction,¹ the role of which strongly increases for heavy atoms (with large Z). The reason is that there is a certain probability for the outer electron to approach the nucleus and thus to see the very strong electric field produced by the unscreened nuclear charge $+Ze$ at the center. Due to the spin–orbit interaction, any electric field acts on the spin of a moving electron.

Being perpendicular both to \mathbf{E} and \mathbf{v} , in an atom the vector \mathbf{B} is normal to the plane of the orbit, thus it is parallel to the orbital angular momentum \mathbf{L} . The energy of the electron magnetic moment in this magnetic field is $\pm\mu_B B$ depending on the orientation of the electron spin (and hence its magnetic moment) with respect to \mathbf{B} (or to \mathbf{L}).²

¹ It is often stated that the origin of the spin–orbit interaction is relativistic and quantum-mechanical. This is true in the sense that it can be derived from the relativistic Dirac equation by keeping terms on the order of $1/c^2$. However, the above formula $\mathbf{B} = (1/c)\mathbf{E} \times \mathbf{v}$ is *not* relativistic: one does not need the theory of relativity to understand that, when moving with respect to a stationary charge, a current, and hence a magnetic field will be seen. Given that the electron has a magnetic moment, the spin–orbit interaction follows directly. It is also not really quantum-mechanical: a classical object having a magnetic moment would experience the same interaction. The only place where quantum mechanics enters is the value of the electron magnetic moment and, of course, the fact that the electron spin is $1/2$.

² In fact the interaction energy derived in this simple-minded way should be cut in half (the “Thomas’s one half” [6]) if one takes properly into account that, because of the electron acceleration in the electric field of the nucleus, its moving frame is not inertial. This finding, made in 1926, resolved the factor of 2 discrepancy between the measured and previously calculated fine structure splittings.

Thus the spin–orbit interaction can be written as $A(\mathbf{L}\mathbf{S})$, the constant A depending on the electron state in an atom. This interaction results in a splitting of atomic levels (the fine structure), which strongly increases for heavy atoms.³

In semiconductors, the spin–orbit interaction depends not only on the velocity of the electron (or its quasi-momentum), but also on the structure of the Bloch functions defining the motion on the atomic scale. As in isolated atoms, it defines the values of the electron g -factors. More details can be found in [7].

Spin–orbit interaction is key to the subject of this book as it enables optical spin orientation and detection (the electrical field of the light wave does not interact directly with the electron spin). It is (in most cases) responsible for spin relaxation. And finally, it makes the transport and spin phenomena inter-dependent.

1.2.4 Hyperfine Interaction with Nuclear Spins

This is the magnetic interaction between the electron and nuclear spins, which may be quite important if the lattice nuclei in a semiconductor have non-zero spin (like in GaAs). If the nuclei get polarized, this interaction is equivalent to the existence of an effective nuclear magnetic field acting on electron spins. The effective field of 100% polarized nuclei in GaAs would be several Tesla!

Because the nuclear magnetic moment is so small (2 000 times less than that of the electron) the equilibrium nuclear polarization at the (experimentally inaccessible) magnetic field of 100 T and a temperature of 1 K would be only about 1%. However, much higher degrees of polarization may be easily achieved through *dynamic nuclear polarization* due to a hyperfine interaction with non-equilibrium electrons.

Experimentally, non-equilibrium nuclear polarization of several percent is easily achieved, recently values up to 50% were observed (see Chap. 11).

Similar to the spin–orbit interaction, the hyperfine interaction may be expressed in the form $A(\mathbf{I}\mathbf{S})$ (the Fermi contact interaction), where \mathbf{I} is the nuclear spin, \mathbf{S} is the electron spin, and the *hyperfine constant* A is proportional to $|\psi(0)|^2$, the square of the electron wave function at the location of the nucleus.

Like spin–orbit interaction, the hyperfine interaction strongly increases in atoms with large Z , and for the same reason. An s -electron in an outer shell has a certain probability to be at the center of the atom, where the nucleus is located, and the nearer it is to the center, the less the nucleus is shielded by the inner electrons. Thus the electron wave function of an s -electron will have a sharp spike in the vicinity of the nucleus. For example, for the In atom the value of $|\psi(0)|^2$ is 6 000 times larger than in the hydrogen atom.

For p -states, and generally for states with $l \neq 0$, the Fermi interaction does not work, since $\psi(0) = 0$, and the electron and nuclear spins are coupled by the much weaker dipole–dipole interaction.

³ Interestingly, general relativity predicts spin–orbit effects (on the order of $(v/c)^2$) in the motion of planets. Thus the “spin” of the Earth should make a slow precession around its orbital angular momentum.

1.2.5 Magnetic Interaction

This is the direct dipole–dipole interaction between the magnetic moments of a pair of electrons. For two electrons located at neighboring sites in a crystal lattice this gives an energy on the order of 1 K. This interaction is normally too weak to be of any importance in semiconductors.

1.3 Basics of Semiconductor Physics

A semiconductor is an insulator with a relatively small forbidden gap and shallow energy levels of electrons bound to impurities. The main feature of a semiconductor is its extreme sensitivity to impurities: a concentration of impurities like one per million of host atoms may determine the electrical conductivity and its temperature dependence.

1.3.1 Electron Energy Spectrum in a Crystal

The potential energy of an electron in a crystal is periodic in space. The most important consequence of this is that the energy spectrum consists of allowed and forbidden energy bands, and that the electron states can be characterized by its quasi-momentum \mathbf{p} (or quasi-wave vector $\mathbf{k} = \mathbf{p}/\hbar$). The energy in an allowed band is a periodic function of \mathbf{k} , so it may be considered only in a certain region of \mathbf{k} -space called the first Brillouin zone. The number of states in an allowed band is equal to twice the number of elementary cells in the crystal (the doubling is due to spin). Thus the energy spectrum is given by the dependence of energy on quasi-momentum, $E(\mathbf{p})$, for all the allowed bands.

In insulators and pure semiconductors at zero temperature a certain number of the lowest allowed bands are completely filled with electrons (according to the Pauli principle), while the higher bands are empty. In most cases only the upper filled band (valence band) and the first empty band (conduction band) are of interest. The conduction and valence bands are separated by a forbidden energy gap of width E_g . In semiconductors the value of E_g may vary from zero (so-called gapless semiconductors, like HgTe) to about 2–3 eV. For Si $E_g \approx 1.1$ eV, for GaAs $E_g \approx 1.5$ eV.

1.3.2 Effective Masses of Electrons and Holes

The important property of semiconductors is that the number of free carriers (electrons in the conduction band or holes in the valence band) is always small compared to the number of atoms. The carriers are produced either by thermal excitation, in which case one has an equal number of electrons and holes, or by doping (see Sect. 1.3.4). Whatever the case, the carrier concentration never exceeds 10^{20} cm^{-3} (normally much less than that), while the number of states per cm^3 in a given band is on the order of 10^{22} , which is also a typical electron concentration in a metal. This means that electrons occupy only a very small fraction of the conduction band where

their energy is lowest (and holes occupy only a very small fraction of the valence band). Consequently, when dealing with a semiconductor, we should be mostly interested in the properties of the energy spectrum in the vicinity of the minimum of the function $E(\mathbf{p})$ for the conduction band and in the vicinity of its maximum for the valence band. If these extrema correspond to the center of the Brillouin zone ($\mathbf{p} = 0$), as it is the case for GaAs and many other materials, then for small \mathbf{p} the function $E(\mathbf{p})$ should be parabolic:

$$E_c = \frac{p^2}{2m_c} \quad \text{for the conduction band,}$$

$$E_v = -\frac{p^2}{2m_v} \quad \text{for the valence band.}$$

Here m_c and m_v are the effective masses of electrons and holes, respectively. The effective masses may differ considerably from the free electron mass m_0 , for example in GaAs $m_c = 0.067m_0$. Generally, the extrema of $E(\mathbf{p})$ do not necessarily occur at the center of the Brillouin zone, also the effective mass may be anisotropic, i.e., have different values for different directions in the crystal.

1.3.3 The Effective Mass Approximation

The effective masses were initially introduced just as convenient parameters to describe the curvature of the $E(\mathbf{p})$ parabolic dependence in the vicinity of its minimum or maximum. However this concept has a more profound meaning. In many cases we are interested in what happens to an electron, or a hole, under the action of some external forces due to, for example, electric and magnetic fields, deformation of the crystal, etc.

It can be shown, that if the spatial variation of these forces is much slower than that of the periodic crystal potential and if the carrier energy remains small compared to the forbidden gap, E_g , we can forget about the existence of the periodic potential and consider our electrons (or holes) as free particles moving in this external field. The only difference is that they have an *effective mass*, not the free electron mass. Thus the classical motion of a conduction electron in an electric field \mathbf{E} and a magnetic field \mathbf{B} is described by the conventional Newton's law: $m_c d^2\mathbf{r}/dt^2 = -e\mathbf{E} - (e/c)\mathbf{v} \times \mathbf{B}$. In particular, the cyclotron frequency of an electron rotating in a magnetic field is determined by the effective mass m_c , and this gives a valuable method of determining the effective masses experimentally (the cyclotron resonance).

If quantum treatment is needed, one can use the Schrödinger equation for an electron in the external field with its effective mass, *forgetting* about the existence of the crystal periodic potential.

Clearly, the validity of the effective mass approximation simplifies enormously the understanding of various physical phenomena in semiconductors.

1.3.4 Role of Impurities

Consider a crystal of germanium in which each atom is linked to its first neighbors by 4 tetrahedral bonds (Ge is an element of column IV of the Periodic Table, it has four electrons to form bonds). Replace one of the host atoms by an atom of As, which belongs to column V. Arsenic will give four of its valence electrons to participate in bonding, and give its remaining fifth electron to the conduction band of the crystal. Thus, arsenic is a *donor* for germanium. The extra electron can travel far away from the donor, which then has a positive charge. Alternatively, the electron may be bound by the positive charge of the donor forming a hydrogen-like “atom”.

If the binding energy is small compared to E_g , and if the effective Bohr radius a_B^* is large compared to the lattice constant, this bound state can be studied using the effective mass approximation described in the previous section. This means that we can use the theory of the hydrogen atom and simply replace in all final formulas the free electron mass m_0 by the effective mass m_c . There is also another simple modification, which takes into account the static dielectric constant of the material, ϵ . The Coulomb potential energy of two opposite charges in vacuum is $-e^2/r$, while inside a polarizable medium it should be replaced by $-e^2/(\epsilon r)$. The ionization energy and the Bohr radius for the hydrogen atom are, respectively: $E_0 = m_0 e^4 / (2\hbar) = 13.6 \text{ eV}$, $a_B = \hbar^2 / (m_0 e^2) \sim 10^{-8} \text{ cm}$. To obtain the corresponding values for an electron bound to a donor in a semiconductor, we make the replacements: $m_0 \rightarrow m_c$, $e^2 \rightarrow e^2/\epsilon$.

Suppose, for example, that $m_c = 0.1m_0$ and $\epsilon = 10$, which are typical values for a semiconductor. Then our electron bound to a donor will have an ionization energy smaller by a factor of 1000 ($E_0^* \sim 10 \text{ meV}$) and an effective Bohr radius larger by a factor of 100 ($a_B^* \sim 10 \text{ nm}$) than the corresponding values for a hydrogen atom. This justifies the validity of the effective mass approximation. It is interesting that within the electron orbit there are roughly 10^5 host atoms! The electron simply does not see these atoms, their only role being to change the free electron mass to m_c . Because of the small value of the binding energy E_0^* , the donor is very easily ionized at moderate temperatures.

Conversely, if we replace the Ge atom by a group III impurity, like gallium, which has three valence electrons, it will take the fourth electron, needed to form the tetrahedral bonds, from the Ge valence band. Then the Ga *acceptor* will become a negatively charged center and a positively charged hole will appear in the valence band. Now the same story applies to the hole: it can either be free, or it may be bound to the negative acceptor forming a hydrogen-like state. It is the effective mass of the hole, m_v , which will now define the ionization energy and the effective Bohr radius. Since in most cases $m_v > m_c$, the acceptor radius is normally smaller than the donor radius, and the ionization of acceptors occurs at higher temperatures. Some complications of this simple picture arise if the effective mass is anisotropic.

Semiconductors are always, either intentionally or non-intentionally, *doped* by impurities and may be *n*-type or *p*-type depending on the dominant impurity type.

1.3.5 Excitons

An exciton in a semiconductor is a bound state of an electron and hole. It is again a hydrogen-like system with properties similar to an electron bound to a donor impurity. The important difference is that an exciton as a whole can move inside the crystal. Another difference is that excitons practically never exist in conditions of equilibrium. Usually they are created by optical excitation. Excitons have a certain lifetime with respect to recombination, during which the bound electron–hole pair annihilates. They can be seen as an absorption line somewhat below E_g .

1.3.6 The Structure of the Valence Band. Light and Heavy Holes

The allowed bands in crystals may be thought of as originating from discrete atomic levels, which are split to form a band when isolated atoms become close to each other. However atomic levels are generally degenerate, i.e., there may be several distinct states having the same energy. This degeneracy may have important consequences for the band energy spectrum of a crystal.

Neglecting Spin–Orbit Interaction

We now restrict the discussion to cubic semiconductors and at first do not consider spin effects. The $\mathbf{p} = 0$ conduction band state is s -type ($l = 0$), the corresponding valence band state is p -type ($l = 1$) and is triply degenerate ($m_l = 0, \pm 1$). Here l is the atomic orbital angular momentum, and m_l is its projection on an arbitrary axis. The problem is to construct an effective mass description of the valence band structure taking into account this threefold degeneracy. This may be done using symmetry considerations: we have a vector \mathbf{p} and a pseudo-vector of angular momentum \mathbf{L} (which is a set of 3×3 matrices $L_x, L_y,$ and L_z , corresponding to $l = 1$, L_z is a diagonal matrix with eigenvalues 1, 0, and -1), and a scalar Hamiltonian should be constructed, which must be quadratic in \mathbf{p} .

If we require invariance under rotations, the only possibility is the Luttinger Hamiltonian [8]:

$$H = Ap^2\mathcal{I} + B(\mathbf{p}\mathbf{L})^2, \quad (1.1)$$

where A and B are arbitrary constants, \mathcal{I} is a unit 3×3 matrix.

Thus the Hamiltonian H is also a 3×3 matrix, and the energy spectrum in the valence band should be found by diagonalizing this matrix. We can greatly simplify this procedure by noting that the choice of the axes x, y, z is arbitrary. Accordingly, we can choose the direction of the z -axis along the vector \mathbf{p} (naturally, the final result does not depend on how the axes are chosen). Then $(\mathbf{p}\mathbf{L})^2 = p^2L_z^2$, so that H becomes diagonal with eigenvalues

$$E_h(p) = (A + B)p^2 \quad \text{for } L_z = \pm 1, \quad E_1(p) = Ap^2 \quad \text{for } L_z = 0.$$

Thus the valence band energy spectrum has two parabolic branches, $E_h(p)$ and $E_1(p)$, the first one being two-fold degenerate. We can now introduce two effective masses, m_h and m_1 , by the relations: $A + B = 1/(2m_h)$ and $A = 1/(2m_1)$ and

say that we have two types of holes in the valence band, the *light* and *heavy* holes (usually $B < 0$, but $A + B > 0$). The difference between these particles is that the heavy hole has a projection of its orbital momentum \mathbf{L} on the direction of \mathbf{p} (*helicity*) equal to ± 1 , while the light hole has a projection equal to 0.

Effects of Spin–Orbit Interaction

If we now include spin but do not take into account the spin–orbit interaction, this will simply double all the states, both in the conduction band and in the valence band. However the spin–orbit interaction essentially changes the energy spectrum of the valence band.

We start again with the atomic states from which the bands originate. The spin–orbit interaction results in an additional energy proportional to $(\mathbf{L}\mathbf{S})$ (see Sect. 1.2.3). Because of this, \mathbf{L} and \mathbf{S} are no longer conserved separately, but only the total angular momentum $\mathbf{J} = \mathbf{L} + \mathbf{S}$.

The eigenvalues of J^2 are $j(j + 1)$ with $|l - s| \leq j \leq l + s$. Thus the state with $l = 0$ (from which the conduction band is built) is not affected ($j = s = 1/2$), while the state with $l = 1$ (from which the valence band is built) is split into two states with $j = 3/2$ and $j = 1/2$. In atomic physics this splitting leads to the fine structure of spectral lines.

The symmetry properties of band states at $\mathbf{p} = 0$ are completely similar to those of the corresponding atomic states. Thus for $\mathbf{p} = 0$ we must have a four-fold degenerate state ($j = 3/2$, $J_z = +3/2, +1/2, -1/2, -3/2$), which is separated by an energy distance Δ , the *spin–orbit splitting*, from a doubly degenerate state ($j = 1/2$, $J_z = +1/2, -1/2$). The conduction band remains doubly degenerate. The value of Δ is small for materials with light atoms, like Si, and may be quite large (comparable to E_g) in semiconductors composed of heavy atoms, like InSb (see Sect. 1.2.3). In GaAs $\Delta \approx 0.3$ eV.

To see what happens to the $j = 3/2$ state for $\mathbf{p} \neq 0$ for energies $E(\mathbf{p}) \ll \Delta$ we construct the Luttinger Hamiltonian in a way quite similar to the procedure in the previous section. The only difference is that the 3×3 matrices L_x , L_y , and L_z , corresponding to $l = 1$, should now be replaced by 4×4 matrices J_x , J_y , and J_z , corresponding to $j = 3/2$:

$$H = Ap^2\mathcal{I} + B(\mathbf{p}\mathbf{J})^2, \quad (1.2)$$

where now \mathcal{I} is a unit 4×4 matrix, the matrix J_z is diagonal with eigenvalues $3/2$, $1/2$, $-1/2$, and $-3/2$.

Proceeding as above, we obtain the spectrum of the heavy and light holes, which is valid for energies much less than Δ :

$$E_h(\mathbf{p}) = \left(A + \frac{9B}{4} \right) p^2 = \frac{p^2}{2m_h} \quad (J_z = \pm 3/2) \quad \text{heavy hole band};$$

$$E_l(\mathbf{p}) = \left(A + \frac{B}{4} \right) p^2 = \frac{p^2}{2m_l} \quad (J_z = \pm 1/2) \quad \text{light hole band}.$$

Both bands are doubly degenerate. Heavy holes have projection of the angular momentum \mathbf{J} on the direction of \mathbf{p} (or helicity) equal to $\pm 3/2$, while for light holes the helicity is $\pm 1/2$. Normally $B < 0$, but $A + 9B/4 > 0$, so that both masses are positive.

The combined description of all three bands (light, heavy, and split-off) on the energy scale $\Delta \sim E(p) \ll E_g$, including effects of non-parabolicity, can be found in [9].

Gapless Semiconductors

Interestingly, the signs of the expressions $A + 9B/4$ and $A + B/4$ may be opposite, which is the case of the so-called gapless semiconductors, like HgTe. In these materials the light hole mass becomes negative, so that this band becomes a conduction band. The conduction band and the valence band (which now consists of heavy holes only) are degenerate at $\mathbf{p} = 0$, so that the energy gap is absent.

Warping of the Iso-energetic Surfaces

Also, it should be noted that the Luttinger Hamiltonian (1.2) presents the so-called spherical approximation: it is invariant under arbitrary rotations. In a cubic crystal the symmetry is generally lower. Thus the true Luttinger Hamiltonian should have a more general form:

$$H = Ap^2\mathcal{I} + B(\mathbf{p}\mathbf{J})^2 + C(J_x^2 p_x^2 + J_y^2 p_y^2 + J_z^2 p_z^2), \quad (1.3)$$

where now the x, y, z axes are not arbitrary, they coincide with the crystallographic axes. The last term makes the iso-energetic surfaces of light and heavy holes anisotropic, so that the energy branches $E_h(\mathbf{p})$ and $E_l(\mathbf{p})$ will not have the simple parabolic form given above. (A similar term should be added to (1.1).)

Oddities in the Behavior of Light and Heavy Holes

In the valence band the “spin” of light and heavy holes is tightly bound to their momentum, and this has many interesting consequences. If some external forces exist, the light and heavy hole states generally become mixed. A simple example is the reflection from an interface.

Suppose that a heavy hole is incident on an ideal flat potential wall. If the incidence is normal, nothing very interesting happens, except that the initial state with helicity $+3/2$ (angular momentum \mathbf{J} parallel to \mathbf{p}) will be transformed after reflection into a state with opposite helicity: $-3/2$. This can be explained by noting that while the initial momentum \mathbf{p} changes sign under reflection, the internal angular momentum remains unchanged.

However for an arbitrary angle of incidence the same reasoning tells us that the reflected heavy hole will have a certain arbitrary angle between \mathbf{J} and \mathbf{p} . But such

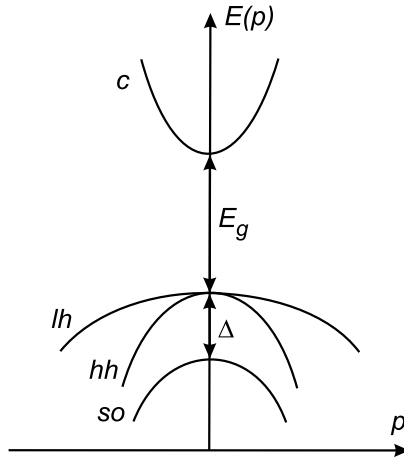


Fig. 1.1. Band structure of GaAs near the center of the Brillouin zone $p = 0$. *c*: conduction band; *hh*: heavy hole band; *lh*: light hole band; *so*: split-off band

free states do not exist! This means that the incident heavy hole will be partly transformed into the light hole. (A similar phenomenon of transformation between ordinary and the extraordinary waves during reflection is known in optics of uniaxial crystals.)

One can reconsider all the textbook problems of quantum mechanics (potential well, tunnel effect, the hydrogen problem, movement in magnetic field, etc.) for a particle, described by the Luttinger Hamiltonian; and these exercises reveal the rather bizarre physics of light and heavy holes in a semiconductor.

1.3.7 Band Structure of GaAs

The above considerations lead to the band structure presented in Fig. 1.1. Near the center of the Brillouin zone there is a simple isotropic conduction band, which is doubly degenerate in spin (for the moment we neglect the spin splitting, see Sect. 1.4.2). The valence band, consists of the sub-bands of light and heavy holes, which are anisotropic (see Sect. 1.3.6), and the isotropic split-off band, which are all doubly degenerate.

1.3.8 Photo-generation of Carriers and Luminescence

In the process of interband absorption of a photon with energy $\hbar\omega > E_g$ in a semiconductor, an electron in the conduction band and a hole in the valence band are generated. During the process the (quasi)momentum is conserved, however the photon momentum $\hbar k = 2\pi\hbar/\lambda$, where λ is the photon wavelength, is very small (compared, for example, to the electron thermal momentum) and normally may be neglected.

In this approximation the optical transitions are *vertical*: to see what happens, we must simply apply a vertical arrow of length $\hbar\omega$ to Fig. 1.1, so that the arrow touches one of the valence bands and the conduction band. The ends of the arrow will give us the initial energies of the generated electrons and holes. An electron may be created in company with a heavy hole, or a light hole; for $\hbar\omega > E_g + \Delta$ the electron-hole pair can also involve a hole in the split-off band. Note, that for a given photon energy the initial electron energy will be different for these three processes.

The photoexcited carriers live some time τ before recombination, which may be radiative (i.e., accompanied by photon emission, which results in luminescence), or non-radiative. In direct-band semiconductors, like GaAs, the recombination is predominantly radiative with a lifetime on the order of 1 ns.

It is important to realize that this time is normally very long compared to the carriers thermalization time. Thermalization means energy relaxation of carriers in their respective bands due to phonon emission and absorption, which results in an equilibrium Boltzmann (or Fermi, depending on temperature and concentration) distribution function of electrons and holes. Thermal equilibrium *between* electrons and holes is established by recombination, on the time scale τ .

Because the recombination time τ is so long compared to the energy relaxation time, the luminescence is produced mostly by thermalized carriers and the emitted photons have energies close to the value of E_g , irrespective of the energy of exciting photons.⁴

It should be noted that semiconductors are normally either intentionally, or non-intentionally doped by impurities. In a *p*-type semiconductor at moderate excitation power the number of photo-generated holes is small compared to the number of equilibrium holes, so that the photo-created electron will recombine with these equilibrium holes, rather than with photo-generated ones.

1.3.9 Angular Momentum Conservation in Optical Transitions

This section is most important for our subject. Along with energy and momentum conservation, the conservation of the angular momentum is a fundamental law of physics. Just like particles, electromagnetic waves have angular momentum. Photons of right or left polarized light have a projection of the angular momentum on the direction of their propagation (helicity) equal to $+1$ or -1 , respectively (in units of \hbar). Linearly polarized photons are in a superposition of these two states.

When a circularly polarized photon is absorbed, this angular momentum is distributed between the photo-excited electron and hole according to the selection rules determined by the band structure of the semiconductor. Because of the complex nature of the valence band, this distribution depends on the value of the momentum of the created electron-hole pair (\mathbf{p} and $-\mathbf{p}$). However, it can be shown that if we take the average over the directions of \mathbf{p} , the result is the same as in optical transitions

⁴ A small part of the excited electrons can emit photons *before* losing their energy by thermalization. The studies of the spectrum and polarization properties of this so-called *hot luminescence* reveal interesting and unusual physics, see [10, 11].

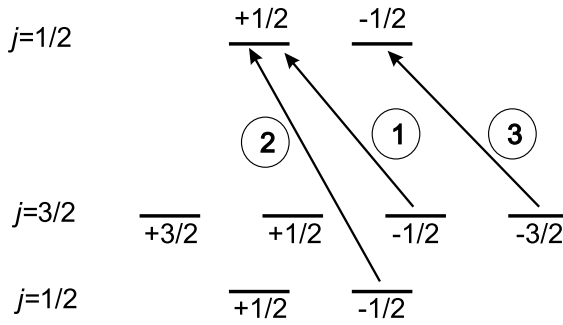


Fig. 1.2. Optical transitions between levels with $j = 3/2$ and $j = 1/2$ (the bands of light and heavy holes, and the split-off band) and the levels with $j = 1/2$ (the conduction band) during an absorption of a right-polarized photon. The probability ratio for the three transitions is 3:2:1

between atomic states with $j = 3/2, m_j = -3/2, -1/2, +1/2, +3/2$ (corresponding to bands of light and heavy holes) and $j = 1/2, m_j = -1/2, +1/2$ (corresponding to the conduction band), see Sect. 1.4.1 below.

Possible transitions between these states, as well as between states in the split-off band and the conduction band, for absorption of a right circularly polarized photon with corresponding relative probabilities are presented in Fig. 1.2. Note, that if we add up *all* transitions, which is the correct thing to do if the photon energy sufficiently exceeds $E_g + \Delta$ the two spin states in the conduction band will be populated equally. This demonstrates the role of spin-orbit interaction for optical spin pumping, see [9, 14] for the details of photon energy dependence of the spin polarization.

1.3.10 Low Dimensional Semiconductor Structures

The development of semiconductor physics in the last two decades is mainly related to studies of artificially engineered low dimensional semiconductor structures, two-dimensional (quantum wells), one-dimensional (quantum wires), and zero-dimensional (quantum dots). By growing a structure consisting of a thin semiconductor layer, for example GaAs, surrounded by material with a larger band gap, for example a solid solution GaAlAs, one obtains a potential well for electrons (and for holes) with a typical width of 20–200 Å.

Thus the first problem in quantum mechanics courses, a particle in a one-dimensional rectangular potential well, which since 1926 was tackled by generations of students as the simplest training exercise, has finally become relevant to some reality!

Energy Spectrum of Electrons and Holes in a Quantum Well

The motion in the direction perpendicular to the layer (the *growth direction*), z , is quantized in accordance with textbooks, while the motion in the plane of the layer xy is unrestrained. Thus the energy spectrum of an electron in a quantum well consists

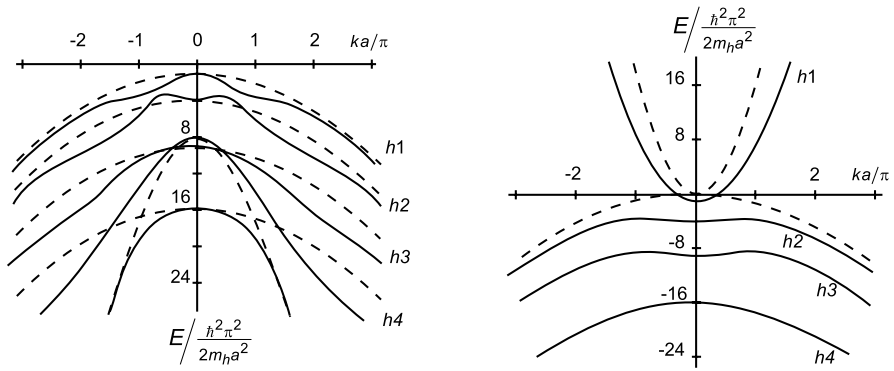


Fig. 1.3. The energy spectrum $E(k)$ of holes (*left*) and of carriers in a gapless semiconductor (*right*) in an infinite rectangular quantum well within the spherical approximation [12]. *Dashed lines* represent the spectrum that would exist if the two types of carriers were independent particles

of two-dimensional *sub-bands*: $E_n(\mathbf{p}) = E_n^0 + p^2/(2m)$, where E_n^0 are the energy levels for the one-dimensional motion in the z direction, \mathbf{p} is the two-dimensional (quasi)momentum in the xy plane, and m is the electron effective mass.

In most cases the electron concentration in the well is such that only the lowest sub-band is occupied. The motion of such electrons is purely two-dimensional (2D). One important consequence is that in an applied magnetic field perpendicular to the 2D plane the spectrum becomes discrete: it consists of Landau levels. A magnetic field parallel to the 2D plane has no effect on the orbital motion of electrons, however it has the usual influence on their spins.

For the case of holes in a quantum well, the problem is not so simple. For $\mathbf{p} = 0$ one has two independent ladders of levels for heavy and light holes, given (for an infinite well) by the textbook formula $E_n^0 = (\pi n \hbar)^2 / (2ma^2)$, where m is the respective effective mass, a is the well width, and $n = 1, 2, 3, \dots$. However, for $\mathbf{p} \neq 0$ the spectrum is determined by the mutual transformations of light and heavy holes during reflections from the potential walls, see Sect. 1.3.6.

Figure 1.3 shows the spectrum of holes and of carriers in a gapless semiconductor in an infinite quantum well calculated in [12] within the spherical approximation (1.2).⁵

Especially interesting is the case of a gapless semiconductor. In a quantum well, a gap will obviously appear due to quantization of the transverse motion. Naively, one would expect this gap to be $E_{e1}^0 - E_{h1}^0 = (1/2)(\pi \hbar/a)^2 / (1/m_e - 1/m_h)$, i.e., mostly determined by the small electron mass. In fact, this is not true, because the

⁵ More accurately, one should use the Hamiltonian in (1.3), which takes care of the warping of iso-energetic surfaces. In fact, the energy spectrum depends on the growth direction, and on the orientation of the vector \mathbf{p} in the xy plane with respect to the crystal axes. However the general properties of the spectrum are the same.

$h1$ sub-band, originating from the first hole level at $p = 0$, becomes *electronic* (see Fig. 1.3). Thus the gap is $\approx m_e/m_h \sim 1/10$ times smaller than expected.

For $pa/\hbar \gg 1$ the first electronic sub-band $h1$ corresponds to *surface states* localized near the well boundaries. Such states should exist also near the surface of a bulk gapless semiconductor [13].

In fact, it is not even necessary to have a sandwich structure to obtain 2D electrons. A simple interface between two different materials plus an electric field of ionized donors gives the same effect, except that now the quantum well is not rectangular, but more like triangular, and that its shape depends on the electron concentration.

The heterostructure design allows to accomplish what was impossible in bulk semiconductors: a spatial separation of the electrons and the donors, from which they originate. The technique of *delta doping* provides a 2D electron gas with previously unimaginable mobilities on the order of 10^7 V/cm² s.

Quantum Dots

Quantum dots are zero-dimensional structures, a sort of large artificial atoms. Under certain growth conditions, *self-assembled* quantum dots appear spontaneously. Typically, they have the form of a flat cake with a height ~ 30 Å and a base diameter of ~ 300 Å. They are embedded in a different material, so that there is a large potential barrier at the interface.

Normally, samples contain an ensemble of many quantum dots with varying parameters, however special techniques allow us to deal with individual dots. Like in an atom, the energy spectrum is discrete. A quantum dot may contain a few electrons or holes.

1.4 Overview of Spin Physics in Semiconductors

The basic ideas concerning spin phenomena in semiconductors were developed both theoretically and experimentally more than 30 years ago. Some of these ideas have been rediscovered only recently. A review of non-equilibrium spin physics in bulk semiconductors can be found in [14], as well as in other chapters of the *Optical Orientation* book.

1.4.1 Optical Spin Orientation and Detection

To date, the most efficient way of creating non-equilibrium spin orientation in a semiconductor is provided by an interband absorption of circularly polarized light.

It can be seen from Fig. 1.2 that for $E_g < \hbar\omega < E_g + \Delta$ absorption produces an average electron spin along the direction of excitation equal to $(-1/2)(3/4) + (+1/2)(1/4) = -1/4$ and an average hole spin equal to $+5/4$, with a sum $+1$, equal to the angular momentum of the absorbed right circularly polarized photon. Thus in a

p-type semiconductor the degree of spin polarization of the photo-excited electrons will be -50% ; the minus sign indicating that the spin orientation is opposite to the angular momentum of incident photons.

If our electron immediately recombines with its partner hole, a 100% circularly polarized photon will be emitted. However in a *p*-type semiconductor electrons will predominantly recombine with the majority holes, which are not polarized. Then the same selection rules show that the circular polarization of luminescence should be $\mathcal{P}_0 = 25\%$, if the holes are not polarized, and if no electron spin relaxation occurs during the electron lifetime τ , i.e., if $\tau_s \gg \tau$. Generally, the degree \mathcal{P} of circular polarization of the luminescence excited by circularly polarized light is less than \mathcal{P}_0 :

$$\mathcal{P} = \frac{\mathcal{P}_0}{1 + \tau/\tau_s}. \quad (1.4)$$

In an optical spin orientation experiment a semiconductor (usually *p*-type) is excited by circularly polarized light with $\hbar\omega > E_g$. The circular polarization of the luminescence is analyzed, which gives a direct measure of the electron spin polarization. Actually, the degree of circular polarization is simply equal to the average electron spin. Thus various spin interactions can be studied by simple experimental means. The electron polarization will be measured provided the spin relaxation time τ_s is not very short compared to the recombination time τ , a condition, which often can be achieved even at room temperature.

1.4.2 Spin Relaxation

Spin relaxation, i.e., disappearance of initial non-equilibrium spin polarization, is the central issue for all spin phenomena. Spin relaxation can be generally understood as a result of the action of fluctuating in time magnetic fields. In most cases, these are not real magnetic fields, but rather “effective” magnetic fields originating from the spin–orbit, or, sometimes, exchange interactions, see Sect. 1.2.

Generalities

A randomly fluctuating magnetic field is characterized by two important parameters: its amplitude (or, more precisely, its rms value), and its correlation time, τ_c , i.e., the time during which the field may be roughly considered as constant. Instead of the amplitude, it is convenient to use the rms value of the spin precession frequency in this random field, ω .

Thus we have the following physical picture of spin relaxation: the spin makes a precession around the (random) direction of the effective magnetic field with a typical frequency ω and during a typical time τ_c . After a time τ_c the direction and the absolute value of the field change randomly, and the spin starts its precession around the new direction of the field. After a certain number of such steps the initial spin direction will be completely forgotten.

How this happens depends on the value of the dimensionless parameter $\omega\tau_c$, which is the typical angle of spin precession during the correlation time. Two limiting cases may be considered:

$\omega\tau_c \ll 1$ (*Most Frequent Case*)

The precession angle is small, so that the spin vector experiences a slow angular diffusion. During a time t , the number of random steps is t/τ_c , for each step the squared precession angle is $(\omega\tau_c)^2$. These steps are not correlated, so that the total squared angle after a time t is $(\omega\tau_c)^2(t/\tau_c)$. The spin relaxation time may be defined as the time at which this angle becomes of the order of 1. Hence,

$$\frac{1}{\tau_s} \sim \omega^2\tau_c. \quad (1.5)$$

This is essentially a *classical* formula (the Planck constant does not enter), although certainly it can be also derived quantum-mechanically. Note, that in this case $\tau_s \gg \tau_c$.

$\omega\tau_c \gg 1$

This means that during the correlation time the spin will make many rotations around the direction of the magnetic field. During the time on the order of $1/\omega$ the spin projection transverse to the random magnetic field is (on the average) completely destroyed, while its projection along the direction of the field is conserved. At this stage the spin projection on its initial direction will diminish three times. [Let the random magnetic field have an angle θ with the initial spin direction. After many rotations the projection of the spin on the initial direction will diminish as $(\cos\theta)^2$. In three dimensions, the average of this value over the possible orientations of the random field yields $1/3$.]

After time τ_c the magnetic field changes its direction, and the initial spin polarization will finally disappear. Thus in the case $\omega\tau_c \gg 1$ the time decay of spin polarization is not exponential, and the process has two distinct stages: the first one has a duration $1/\omega$, and the second one has a duration τ_c . The overall result is $\tau_s \sim \tau_c$.

This consideration is quite general and applies to any mechanism of spin relaxation. We have only to understand the values of the relevant parameters ω and τ_c for a given mechanism.

Spin Relaxation Mechanisms

There are several possible mechanisms providing the fluctuating magnetic fields responsible for spin relaxation.

Elliott–Yafet Mechanism [15, 16]

The electrical field, accompanying lattice vibrations, or the electric field of charged impurities is transformed to an effective magnetic field through a spin–orbit interaction. Thus momentum relaxation should be accompanied by spin relaxation.

For phonons, the correlation time is on the order of the inverse frequency of a typical thermal phonon. Spin relaxation by phonons is normally rather weak, especially at low temperatures.

For scattering by impurities, the direction and the value of the random magnetic field depends on the geometry of the individual collision (the impact parameter). This random field cannot be characterized by a single correlation time, since it exists only *during* the brief act of collision and is zero between collisions. In each act of scattering the electron spin rotates by some small angle ϕ . These rotations are uncorrelated for consequent collisions, so the average square of spin rotation angle during time t is on the order of $\langle \phi^2 \rangle (t/\tau_p)$, where τ_p is the time between collisions and $\langle \phi^2 \rangle$ is the average of ϕ^2 over the scattering geometry.

Thus $1/\tau_s \sim \langle (\phi)^2 \rangle / \tau_p$. The relaxation rate is obviously proportional to the impurity concentration.

Dyakonov–Perel Mechanism [9, 17]

This one is related to the spin–orbit splitting of the conduction band in non-centrosymmetric semiconductors like GaAs (but not Si or Ge, which are centrosymmetric). For bulk semiconductors, this splitting was first pointed out by Dresselhaus [18]. The additional spin-dependent term in the electron Hamiltonian can be presented as

$$\hbar \boldsymbol{\Omega}(\mathbf{p}) S, \quad (1.6)$$

which can be viewed as the energy of a spin in an effective magnetic field. Here $\boldsymbol{\Omega}(\mathbf{p})$ is a vector depending on orientation of the electron momentum with respect to the crystal axes (xyz), such that

$$\Omega_x \sim p_x(p_y^2 - p_z^2), \quad \Omega_y \sim p_y(p_z^2 - p_x^2), \quad \Omega_z \sim p_z(p_x^2 - p_y^2). \quad (1.7)$$

For a given \mathbf{p} , $\boldsymbol{\Omega}(\mathbf{p})$ is the spin precession frequency in this field. This frequency is proportional to $p^3 \sim E^{3/2}$. The effective magnetic field changes in time because the direction of \mathbf{p} varies due to electron collisions. Thus the correlation time is on the order of the momentum relaxation time, τ_p , and if $\boldsymbol{\Omega} \tau_p$ is small, which is normally the case, we get

$$\frac{1}{\tau_s} \sim \boldsymbol{\Omega}^2 \tau_p. \quad (1.8)$$

In contrast to the Elliott–Yafet mechanism, now the spin rotates not during, but *between* the collisions. Accordingly, the relaxation rate *increases* when the impurity concentration decreases (i.e., when τ_p becomes longer). It happens that this mechanism is often the dominant one, both in bulk A^{III}B^V and A^{II}B^{VI} semiconductors, like GaAs and in 2D structures (where $\boldsymbol{\Omega}(\mathbf{p}) \sim p$, see below).

Bir–Aronov–Pikus Mechanism [19]

This is a mechanism of spin relaxation of non-equilibrium electrons in p -type semiconductors due to the exchange interaction between the electron and hole spins (or, expressing it otherwise, exchange interaction between an electron in the conduction band and all the electrons in the valence band). This spin relaxation rate, being proportional to the number of holes, may become the dominant one in heavily p -doped semiconductors.

Relaxation via Hyperfine Interaction with Nuclear Spins

The electron spin interacts with the spins of the lattice nuclei (see Sect. 1.4.5 below), which are normally in a disordered state. Thus the nuclei provide a random effective magnetic field, acting on the electron spin. The corresponding relaxation rate is rather weak, but may become important for localized electrons, when other mechanisms, associated with electron motion, do not work.

Spin Relaxation of Holes in the Valence Band

The origin of this relaxation is in the splitting of the valence band into sub-bands of light and heavy holes. In this case, $\hbar\Omega(\mathbf{p})$ is equal to the energy difference between light and heavy holes for a given \mathbf{p} and the correlation time is again τ_p . However, in contrast to the situation for electrons in the conduction band, we have now the opposite limiting case: $\Omega(p)\tau_p \gg 1$. So, the hole spin relaxation time is on the order of τ_p , which is very short. One can say that the hole “spin” \mathbf{J} is rigidly fixed with respect to its momentum \mathbf{p} , and because of this, momentum relaxation leads automatically to spin relaxation.

For this reason, normally it is virtually impossible to maintain an appreciable non-equilibrium polarization of bulk holes. However, Hilton and Tang [20] have managed to observe the spin relaxation (on the femtosecond time scale) of both light and heavy holes in undoped bulk GaAs. The general theory of the relaxation of spin, as well as helicity and other correlations between \mathbf{J} and \mathbf{p} , for holes in the valence band was given in [21].

Influence of Magnetic Field on Spin Relaxation

In the presence of an external magnetic field \mathbf{B} , the spins perform a regular precession with a frequency $\Omega = g\mu B/\hbar$, and one should distinguish between relaxation of the spin component along \mathbf{B} and the relaxation, or *dephasing*, of the perpendicular components. In the magnetic resonance literature it is customary to denote the corresponding longitudinal and transverse times as T_1 and T_2 , respectively.

To understand what happens, it is useful to go to a frame rotating around \mathbf{B} with the spin precession frequency Ω . In the absence of random fields, the spin vector would remain constant in the rotating frame. Relaxation is due to random fields in the rotating frame, and obviously these fields now rotate around \mathbf{B} with the same frequency Ω .

Thus random fields directed along \mathbf{B} are the same as in the rest frame, and cause the same relaxation of the perpendicular spin components with a characteristic time $T_2 \sim \tau_s$. However the perpendicular components of the random field, which are responsible for the relaxation of the spin component along \mathbf{B} , do rotate. The importance of this rotation is determined by the parameter $\Omega\tau_c$, the angle of rotation of the random field during the correlation time.

If $\Omega\tau_c \ll 1$, then rotation is of no importance, since the random field will anyway change its direction after a time τ_c . However, for $\Omega\tau_c \gg 1$ the rotating random field

will effectively average out during the correlation time, resulting in a decrease of the longitudinal spin relaxation rate.

A simple calculation gives

$$\frac{1}{T_1} = \frac{1}{\tau_s} \frac{1}{1 + (\Omega\tau_c)^2} = \frac{\omega^2\tau_c}{1 + (\Omega\tau_c)^2}. \quad (1.9)$$

Interestingly, with increasing magnetic field the longitudinal spin relaxation rate changes from being proportional to τ_c to becoming proportional to $1/\tau_c$.

Again, the classical formula (1.9) can be derived quantum mechanically. From the quantum point of view the longitudinal relaxation is due to flips of the spin projection on \mathbf{B} , which requires an energy $g\mu B$. Since the energy spectrum of the random field has a width \hbar/τ_c the process becomes ineffective when $g\mu B \gg \hbar/\tau_c$, or equivalently, when $\Omega\tau_c \gg 1$.

Ivchenko [22] has calculated the influence of magnetic field on the Dyakonov–Perel spin relaxation. The result coincides with (1.9) with $\tau_c = \tau_p$, except that the spin precession frequency Ω is replaced by the (greater) electron cyclotron frequency, ω_c . The reason is that for this case the rotation of the vector $\boldsymbol{\Omega}(\mathbf{p})$ is primarily due to the rotation of the electron momentum \mathbf{p} in the magnetic field.

Spin Relaxation of Two-dimensional Electrons and Holes

Usually the Dyakonov–Perel mechanism is the dominant one. However, the momentum dependence of the effective magnetic field, or the vector $\boldsymbol{\Omega}(\mathbf{p})$, is quite different.

First, because the projection of momentum perpendicular to the 2D plane is quantized and fixed, and because it is usually much greater than the in-plane projections, the spin splitting defined by (1.6) becomes *linear* in the in-plane momentum [23].

For the simplest case when the growth direction is (001), we must replace p_z and p_z^2 in (1.7) by their quantum-mechanical average values in the lowest sub-band, which are equal to 0 and $\langle p_z^2 \rangle$, respectively (for a deep rectangular well of width a , $\langle p_z^2 \rangle = (\pi\hbar/a)^2$). These considerations give

$$\Omega_x \sim -p_x \langle p_z^2 \rangle, \quad \Omega_y \sim p_y \langle p_z^2 \rangle, \quad \Omega_z = 0. \quad (1.10)$$

We see that the effective magnetic field is linear in \mathbf{p} and lies in the 2D plane. As a consequence, the spin relaxation is anisotropic: the spin component perpendicular to the plane decays two times faster than the spin in-plane components.⁶

Thus the spin relaxation of 2D electrons is generally anisotropic and depends on the growth direction [23]. An interesting case is when the growth direction corresponds to (110). If we now take *this* direction as the z axis, and take x and y axes along the in-plane $(1\bar{1}0)$ and (001) directions, respectively, in the same manner as above we obtain

$$\Omega_x = 0, \quad \Omega_y = 0, \quad \Omega_z \sim p_x. \quad (1.11)$$

⁶ The reason is that the z projection of the spin is rotated by both x and y components of the random field, while the x spin projection is influenced only by the y component, since the z component of the random field is zero.

The random effective magnetic field is now always perpendicular to the 2D plane! Its value and sign depend only on the projection of electron momentum on the $(\bar{1}\bar{1}0)$ direction. This means that now the relaxation times for both in-plane components of the spin are equal, however the normal to the plane spin component does not relax at all.⁷

Second, if the quantum well is asymmetric, e.g., the triangular well in a heterostructure, there is another source of effective magnetic field, besides that originating from the Dresselhaus term, (1.7) and (1.6). This is due to the Bychkov–Rashba splitting [25, 26], which has the form (1.6) with

$$\boldsymbol{\Omega}(\mathbf{p}) \sim \mathbf{E}^R \times \mathbf{p}, \quad (1.12)$$

where \mathbf{E}^R is the so-called “Rashba field”, a built-in vector oriented along the growth direction and defined by the asymmetry of the quantum well.⁸ For this case $\boldsymbol{\Omega}$ also lies in the 2D plane and is perpendicular to \mathbf{p} .

Although the $\boldsymbol{\Omega}(\mathbf{p})$ dependence is different from the one considered above for the (001) growth direction, the relaxation process is quite similar. However, if both types of interactions coexist and are of the same order of magnitude, a specific anisotropy of relaxation in the xy plane arises due to a kind of interference between the two terms [28].

The spin structure of holes in a quantum well is also completely different that in the bulk. More details on spin–orbit interaction in two-dimensional systems can be found in Winkler’s book [29].

1.4.3 Hanle Effect

Depolarization of luminescence by a transverse magnetic field (first discovered by Wood and Ellett, as described in Sect. 1.1) is effectively employed in experiments on spin orientation in semiconductors.

The reason for this effect is the precession of electron spins around the direction of the magnetic field. Under continuous illumination, this precession leads to the decrease of the average projection of the electron spin on the direction of observation, which defines the degree of circular polarization of the luminescence. Thus the degree of polarization decreases as a function of the transverse magnetic field. Measuring this dependence under steady state conditions makes it possible to determine both the spin relaxation time and the recombination time.

This effect is due to the precession of electron spins in a magnetic field \mathbf{B} with the Larmor frequency Ω . This precession, along with spin pumping, spin relaxation, and recombination is described by the following simple equation of motion of the

⁷ In fact, the normal spin component *will* slowly decay because of the small cubic in \mathbf{p} terms, which were neglected in deriving (1.10) and (1.11). Experimentally, a ~ 20 times suppression of spin relaxation in (110) quantum wells is observed.

⁸ The corresponding term in the Hamiltonian of 2D electrons was previously derived by Vasko [27].

average spin vector \mathbf{S} :

$$\frac{d\mathbf{S}}{dt} = \boldsymbol{\Omega} \times \mathbf{S} - \frac{\mathbf{S}}{\tau_s} - \frac{\mathbf{S} - \mathbf{S}_0}{\tau}, \quad (1.13)$$

where the first term on the rhs describes spin precession in a magnetic field ($\boldsymbol{\Omega} = g\mu B/\hbar$), the second term describes spin relaxation, and the third one describes generation of spin by optical excitation (\mathbf{S}_0/τ) and recombination ($-\mathbf{S}/\tau$). The vector \mathbf{S}_0 is directed along the exciting light beam, its absolute value is equal to the initial average spin of photo-created electrons.

In the stationary state ($d\mathbf{S}/dt = 0$) and in the absence of a magnetic field, one finds

$$S_z(0) = \frac{S_0}{1 + \tau/\tau_s}, \quad (1.14)$$

where $S_z(0)$ is the projection of the spin on the direction of \mathbf{S}_0 (z -axis). Since $S_z(0)$ is equal to the degree of polarization of the luminescence (Sect. 1.4.1), this formula is equivalent to the expression for \mathcal{P} in (1.4). In the presence of magnetic field transverse to \mathbf{S}_0 we obtain

$$S_z(B) = \frac{S_z(0)}{1 + (\Delta\tau^*)^2}, \quad \frac{1}{\tau^*} = \frac{1}{\tau} + \frac{1}{\tau_s}. \quad (1.15)$$

The effective time τ^* defines the width of the depolarization curve. Thus the spin projection S_z (and hence the degree of circular polarization of the luminescence) decreases as a function of the transverse magnetic field. Combining the measurements of the zero-field value $\mathcal{P} = S_z(0)$ and of the magnetic field dependence in the Hanle effect, we can find the two essential parameters: the electron lifetime, τ , and the spin relaxation time, τ_s , under steady-state conditions.

If polarized electrons are created by a short pulse, time-resolved measurements reveal, very impressively, the damped spin precession around the direction of magnetic field [30], which follows from (1.13) for a given initial spin value.

1.4.4 Mutual Transformations of Spin and Charge Currents

Because of spin-orbit interaction, charge and spin transport are interconnected: an electrical current produces a transverse spin current and vice versa [31, 32]. In recent years this has become a subject of considerable interest and intense research, both experimental and theoretical, see Chap. 8.

One of the new phenomena, predicted in [31, 32] and now called the Spin Hall Effect, consists of the current-induced spin accumulation at the boundaries of a conductor. The spins are perpendicular to the direction of the electric current and have opposite signs on the opposing boundaries.⁹ Accumulation occurs on the spin diffusion length $L_s = \sqrt{D\tau_s}$, where D is the diffusion coefficient. Typically L_s is on the order of 1 μm .

⁹ This is reminiscent of what happens in the normal Hall effect, where *charges* of opposite sign accumulate at the boundaries because of the Lorentz force.

Inversely, a spin current, due for example to the inhomogeneity of the spin density, generates an electric current. More precisely, there is an electric current proportional to curl \mathbf{S} (the Inverse Spin Hall Effect). This effect was found experimentally for the first time by Bakun et al. [33].

In gyrotropic crystals a current can be induced by a *homogeneous* non-equilibrium spin density, as it was shown theoretically by Ivchenko and Pikus [34] and by Belinicher [35]. The first experimental demonstration of this effect was reported in [36]. Inversely, an electric current will generate a uniform spin polarization.

Thus, generally, an electric current can induce spin accumulation at the boundaries, or a uniform spin polarization, or both effects simultaneously. Reciprocal effects exist too.

Phenomenologically, all these effects (including the well-known anomalous Hall effect [37]) can be derived from pure symmetry considerations, according to the general principle: *everything, that is not forbidden by symmetry or conservation laws, will happen*. In an isotropic media with inversion symmetry, the only building block is the unit antisymmetric tensor ϵ_{ijk} . If the symmetry is lower, there will be other tensors, that the theory may use. The microscopic theory should provide the physical mechanism of the phenomenon under consideration, as well as the values of the observable quantities. More details can be found in Chaps. 8 and 9.

1.4.5 Interaction between the Electron and Nuclear Spin Systems

The non-equilibrium spin-oriented electrons can easily transmit their polarization to the lattice nuclei, thus creating an effective magnetic field. This field will, in turn, influence the spin of electrons (but not their orbital motion). For example, it can strongly influence the electron polarization via the Hanle effect [38]. Thus the spin-oriented electrons and the polarized lattice nuclei form a strongly coupled system, in which spectacular non-linear phenomena, like self-sustained slow oscillations and hysteresis are observed by simply looking at the circular polarization of the luminescence [14, 39]. Optical detection of the nuclear magnetic resonance in a semiconductor was demonstrated for the first time by Ekimov and Safarov [40].

The physics of these phenomena are governed by three basic interactions:

Hyperfine Interaction between Electron and Nuclear Spins

The interaction has the form $A(\mathbf{I}\mathbf{S})$, where \mathbf{I} is the nuclear spin and \mathbf{S} is the electron spin. If the electrons are in equilibrium this interaction provides a mechanism for nuclear spin relaxation. If the electron spin system is out of equilibrium, it leads to dynamic nuclear polarization. These processes are very slow compared to the characteristic electron time scale. On the other hand, if the nuclei are polarized, this interaction is equivalent to the existence of an effective nuclear magnetic field. The field of 100% polarized nuclei in GaAs would be about 6 T. Experimentally, nuclear polarization of several percent is easily achieved.

The time of build-up of nuclear polarization due to interaction with electrons is given by the general formula (1.5), where ω should be understood as the precession

frequency of the nuclear spin in the effective electron magnetic field due to hyperfine interaction, and the correlation time τ_c depends on the electron state. For mobile electrons this time is extremely short: $\tau_c \sim \hbar/E$, where E is the electron energy. As first pointed out by Bloembergen [43], nuclear polarization (or depolarization) by electrons is much more effective when the electrons are localized, for example, bound to donors, or confined in a quantum dot. In this case τ_c is generally much longer than for mobile carriers. It is defined by the shortest of processes like recombination, hopping to another donor site, thermal ionization, or spin relaxation.

Dipole–Dipole Interaction between Nuclear Spins

This interaction can be characterized by the local magnetic field, B_L , on the order of several Gauss, which is created at a given nuclear site by the neighboring nuclei.¹⁰ The precession period of a nuclear spin in the local field, on the order of $T_2 \sim 10^{-4}$ s, gives a typical intrinsic time scale for the nuclear spin system. During this time, thermal equilibrium within this system is established, with a *nuclear spin temperature* Θ_N , which may be very different from the crystal temperature T , for example, something like 10^{-6} K.

Since the times characterizing the interaction of the nuclear spin system with the outside world (electrons, or lattice) is much greater than T_2 , the nuclear spin system can be considered as always being in a state of internal thermal equilibrium with a nuclear spin temperature defined by the energy exchange with the electrons and/or the lattice. Accordingly, the nuclear polarization *is always given by the thermodynamic formula* $\mathcal{P} \sim \mu_N B / (k\Theta_N)$, where μ_N is the nuclear magnetic moment. The most important concept of the nuclear spin temperature was introduced by Redfield [41], see also [42].

The dipole–dipole interaction is also responsible for the nuclear spin diffusion [43]—a process that tends to make the nuclear polarization uniform in space. The nuclear spin diffusion coefficient can be estimated as $D_N \sim a_0^2/T_2 \sim 10^{-12}$ cm²/s, where a_0 is the distance between the neighboring nuclei. Thus it takes about 1 s to spread out the nuclear polarization on a distance of 100 Å, and several hours for a distance of 1 μm.

Zeeman Interaction of Electron and Nuclear Spins

The energy of a nuclear magnetic moment in an external magnetic field is roughly 2 000 times smaller than that for the electron. However, it becomes important in magnetic fields exceeding the local field $B_L \sim 3$ G. Accordingly, the behavior of the nuclear spin system in small fields, less than B_L , is quite different than in larger

¹⁰ As was pointed out in Sect. 1.2, the magnetic dipole–dipole interaction between electron spins can be usually neglected. Given that a similar interaction between nuclear spins is about a million times smaller, it may seem strange that this interaction may be of any importance. The answer comes when we consider the extremely long time scale in the nuclear spin system (seconds or more) compared to the characteristic times for the electron spin system (nanoseconds or less).

fields. At zero magnetic field the nuclear spins can not be polarized (the Zeeman energy is zero, while Θ_N remains finite, see the thermodynamic formula above).

Also, as the magnetic field increases, the time of polarization will increase according to (1.9), where Ω is the electron spin precession frequency. Quantum mechanically, this increase is the result of the strong mismatch between the electron and nuclear Zeeman energies. Because of this mismatch the electron–nucleus flip–flop transitions would violate energy conservation. They can occur, however, because of the energy uncertainty $\Delta E \sim \hbar/\tau_c$.

The interplay of these interactions under various experimental conditions accounts for the extremely rich and interesting experimental findings in this domain, see Chap. 11.

1.5 Overview of the Book Content

Within the scope of this introductory chapter it is only possible to briefly outline the main directions of the current research.

Time-Resolved Optical Techniques. The innovative time resolved optical techniques, based on Faraday or Kerr polarization rotation, were developed by Awschalom’s group in Santa Barbara [45] and by Harley’s group in Southampton [46]. These techniques opened a new era in experimental spin physics. They have allowed for the visualization of spin dynamics on the sub-picosecond time scale and study of the intimate details of various spin processes in a semiconductor. This book presents several subjects, where most of the experimental results are obtained by using these optical techniques.

Spin Dynamics in Quantum Wells and Quantum Dots. The spin dynamics of carriers in quantum wells is discussed in Chap. 2. Exciton spin dynamics and the fine structure of neutral and charged excitons are presented in Chaps. 3 (quantum wells) and 4 (quantum dots). The interplay between carrier exchange and confinement leads to quite a number of interesting and subtle effects, that are now well understood. These chapters show how many important parameters, like spin splittings and relaxation times, can be accurately determined.

Spin Noise Spectroscopy. Chapter 5 gives a general introduction to experimental time-resolved techniques. It also presents quite a new way of research in spin physics, where the methods of noise spectroscopy, known in other domains, are applied to the spin system in a semiconductor. Unlike other techniques, this allows for the study of spin dynamics without perturbing the system by an external excitation.

Coherent Spin Dynamics in Quantum Dots. This topic is covered in Chap. 6. It contains extraordinarily interesting and surprising new results on “mode-locking” of spin coherence in an ensemble of quantum dots excited by a periodic sequence of laser pulses and, in particular, on spin precession “focusing” induced by the hyperfine interaction with the nuclear spins.

Spin Properties of Confined Electrons in Silicon. Spin-related studies in silicon were somewhat neglected in recent years, because it practically does not give photoluminescence, has a weak spin-orbit interaction, and contains few nuclear spins. However, Chap. 7 demonstrates interesting new spin physics in Si-based quantum wells and quantum dots, studied mostly by the electron spin resonance, which may have extremely small line-widths.

Coupling of Spin and Charge Currents. Chapter 8 is devoted to the coupling between the spin and charge currents due to spin-orbit interaction and the Spin Hall Effect, which was observed only recently and caused widespread interest. A related subject is treated in Chap. 9 describing spin-related photocurrents, or circular photo-galvanic effect, in two-dimensional structures. There are a variety of interesting experiments, which reveal subtle physics.

Spin Injection. Spin injection from a ferromagnet to a normal metal, originally proposed by Aronov [47], and spin detection using a ferromagnet, originally proposed by Silsbee [48], was first observed by Johnson and Silsbee [49]. Injection through a ferromagnet/semiconductor junction has been investigated in many recent works. Chapter 10 describes these and related phenomena, which have some promising applications.

Nuclear Spin Effects in Optics and Electron Transport. Chapter 11 discusses electron-nuclear spin systems formed by the hyperfine interaction in quantum wells and quantum dots. Nuclear spin polarization results in spectacular optical effects, including unusual magnetic resonances and hysteretic behavior.

Chapter 12 describes some astonishing manifestations of nuclear spins in low temperature magneto-transport in two dimensions, first observed by Dohers et al. [50]. Strong changes of the magnetoresistance in the Quantum Hall Effect regime are observed and shown to be caused by the dynamic nuclear spin polarization. Such studies yield unique insights into the properties of fragile quantum Hall states, which only exist at ultra-low temperatures and in the highest mobility samples. Some of the experimental results still remain to be understood.

Spin Dynamics in Diluted Magnetic Semiconductors. Mn doped III-V and II-VI systems, both bulk and two-dimensional, have attracted intense interest. The giant Zeeman splitting due to exchange interaction with Mn, combination of ferromagnetic and semiconductor properties, and the possibility of making a junction between a ferromagnetic and a normal semiconductor have been the focus of numerous studies. The basic physics, the magnetic and optical properties are reviewed in Chap. 13.

References

- [1] R.W. Wood, A. Ellett, Phys. Rev. **24**, 243 (1924)
- [2] W. Hanle, Z. Phys. **30**, 93 (1924)
- [3] J. Brossel, A. Kastler, C. R. Hebd. Acad. Sci. **229**, 1213 (1949)
- [4] A. Kastler, Science **158**, 214 (1967)
- [5] G. Lampel, Phys. Rev. Lett. **20**, 491 (1968)

- [6] L.H. Thomas, *Nature* **117**, 514 (1926)
- [7] P.Y. Yu, M. Cardona, *Fundamental of Semiconductors*, 3rd edn. (Springer, Berlin, 2001)
- [8] J.M. Luttinger, *Phys. Rev.* **102**, 1030 (1956)
- [9] M.I. Dyakonov, V.I. Perel, *Z. Eksp. Teor. Fiz.* **60**, 1954 (1971); *Sov. Phys. JETP* **33**, 1053 (1971)
- [10] V.D. Dymnikov, M.I. Dyakonov, V.I. Perel, *Z. Eksp. Teor. Fiz.* **71**, 2373 (1976); *Sov. Phys. JETP* **44**, 1252 (1976)
- [11] D.N. Mirlin, in *Optical Orientation*, ed. by F. Meier, B.P. Zakharchenya (North-Holland, Amsterdam, 1984), p. 133
- [12] M.I. Dyakonov, A.V. Khaetskii, *Z. Eksp. Teor. Fiz.* **82**, 1584 (1982); *Sov. Phys. JETP* **55**, 917 (1982)
- [13] M.I. Dyakonov, A.V. Khaetskii, *Pis'ma Z. Eksp. Teor. Fiz.* **33**, 110 (1981); *Sov. Phys. JETP Lett.* **33**, 115 (1981)
- [14] M.I. Dyakonov, V.I. Perel, in *Optical Orientation*, ed. by F. Meier, B.P. Zakharchenya (North-Holland, Amsterdam, 1984), p. 15
- [15] R.J. Elliott, *Phys. Rev.* **96**, 266 (1954)
- [16] Y. Yafet, in *Solid State Physics*, vol. 14, ed. by F. Seits, D. Turnbull (Academic, New York, 1963), p. 1
- [17] M.I. Dyakonov, V.I. Perel, *Fiz. Tverd. Tela* **13**, 3581 (1971); *Sov. Phys. Solid State* **13**, 3023 (1972)
- [18] G. Dresselhaus, *Phys. Rev.* **100**, 580 (1955)
- [19] G.I. Bir, A.G. Aronov, G.E. Pikus, *Z. Eksp. Teor. Fiz.* **69**, 1382 (1975); *Sov. Phys. JETP* **42**, 705 (1976)
- [20] D.J. Hilton, C.L. Tang, *Phys. Rev. Lett.* **89**, 146601 (2002)
- [21] M.I. Dyakonov, A.V. Khaetskii, *Z. Eksp. Teor. Fiz.* **86**, 1843 (1984); *Sov. Phys. JETP* **59**, 1072 (1984)
- [22] E.L. Ivchenko, *Fiz. Tverd. Tela* **15**, 1566 (1973); *Sov. Phys. Solid State* **15**, 1048 (1973)
- [23] M.I. Dyakonov, V.Yu. Kachorovskii, *Fiz. Techn. Poluprov.* **20**, 178 (1986); *Sov. Phys. Semicond.* **20**, 110 (1986)
- [24] Y. Ohno, R. Terauchi, T. Adachi, F. Matsukura, H. Ohno, *Phys. Rev. Lett.* **83**, 4196 (1999)
- [25] Y.A. Bychkov, E.I. Rashba, *J. Phys. C* **17**, 6039 (1984)
- [26] Y.A. Bychkov, E.I. Rashba, *Z. Eksp. Teor. Fiz. Pis'ma*, **39**, 66 (1984); *Sov. Phys. JETP Lett.* **39**, 78 (1984)
- [27] F.T. Vasko, *Z. Eksp. Teor. Fiz. Pis'ma*, **30**, 574 (1979); *Sov. Phys. JETP Lett.* **30**, 541 (1979)
- [28] N.S. Averkiev, L.E. Golub, *Phys. Rev. B* **60**, 15582 (1999)
- [29] R. Winkler, *Spin-Orbit Coupling Effects in Two-dimensional Electron and Hole Systems* (Springer, Berlin, 2003)
- [30] J.A. Gupta, X. Peng, A.P. Alivisatos, D.D. Awschalom, *Phys. Rev. B* **59**, 10421 (1999)
- [31] M.I. Dyakonov, V.I. Perel, *Pis'ma Z. Eksp. Teor. Fiz.* **13**, 657 (1971); *Sov. Phys. JETP Lett.* **13**, 467 (1971)
- [32] M.I. Dyakonov, V.I. Perel, *Phys. Lett. A* **35**, 459 (1971)
- [33] A.A. Bakun, B.P. Zakharchenya, A.A. Rogachev, M.N. Tkachuk, V.G. Fleisher, *Pis'ma Z. Eksp. Teor. Fiz.* **40**, 464 (1984); *Sov. Phys. JETP Lett.* **40**, 1293 (1984)
- [34] E.L. Ivchenko, G.E. Pikus, *Pis'ma Z. Eksp. Teor. Fiz.* **27**, 640 (1978); *Sov. Phys. JETP Lett.* **27**, 604 (1978)
- [35] V.I. Belinicher, *Phys. Lett. A* **66**, 213 (1978)
- [36] V.M. Asnin, A.A. Bakun, A.M. Danishevskii, E.L. Ivchenko, G.E. Pikus, A.A. Rogachev, *Solid State Commun.* **30**, 565 (1979)

- [37] R. Karplus, J.M. Luttinger, *Phys. Rev.* **95**, 1154 (1954)
- [38] M.I. Dyakonov, V.I. Perel, V.I. Berkovits, V.I. Safarov, *Z. Eksp. Teor. Fiz.* **67**, 1912 (1974); *Sov. Phys. JETP* **40**, 950 (1975)
- [39] V.G. Fleisher, I.A. Merkulov, in *Optical Orientation*, ed. by F. Meier, B.P. Zakharchenya (North-Holland, Amsterdam, 1984), p. 173
- [40] A.I. Ekimov, V.I. Safarov, *Pis'ma Z. Eksp. Teor. Fiz.* **15**, 453 (1972); *Sov. Phys. JETP Lett.* **15**, 179 (1972)
- [41] A.G. Redfield, *Phys. Rev.* **98**, 1787 (1955)
- [42] A. Abragam, *The Principles of Nuclear Magnetism* (Oxford University Press, Oxford, 1983)
- [43] N. Bloembergen, *Physica* **20**, 1130 (1954)
- [44] N. Bloembergen, *Physica* **25**, 386 (1949)
- [45] J.J. Baumberg, D.D. Awschalom, N. Samarth, *J. Appl. Phys.* **75**, 6199 (1994)
- [46] N.I. Zheludev, M.A. Brummell, A. Malinowski, S.V. Popov, R.T. Harley, *Solid State Commun.* **89**, 823 (1994)
- [47] A.G. Aronov, *Pis'ma Z. Eksp. Teor. Fiz.* **24**, 37 (1976); *Sov. Phys. JETP Lett.* **24**, 32 (1976)
- [48] R.H. Silsbee, *Bull. Mag. Res.* **2**, 284 (1980)
- [49] M. Johnson, R.H. Silsbee, *Phys. Rev. Lett.* **55**, 1790 (1985)
- [50] M. Dobers, K. von Klitzing, J. Schneider, G. Weinmann, K. Ploog, *Phys. Rev. Lett.* **61**, 1650 (1988)